

**TERNARY HYBRID PVDF-HFP/PANI/GO
POLYMER ELECTROLYTE MEMBRANE FOR
LITHIUM ION BATTERY**

USAID UR REHMAN FAROOQUI

**UNIVERSITI SAINS MALAYSIA
2019**

**TERNARY HYBRID PVDF-HFP/PANI/GO POLYMER
ELECTROLYTE MEMBRANE FOR LITHIUM ION BATTERY**

by

USAID UR REHMAN FAROOQUI

**Thesis submitted in fulfilment of the requirements
for the degree of
Doctor of Philosophy**

April 2019

ACKNOWLEDGEMENT

At first, I would like to thank to almighty Allah for blessing me with such a great opportunity. After that, I would like to show my heartily gratitude to my parents Mr. Mahfooz ur Rehman Farooqui and Miss. Ayesha Begum; also, to my wife Miss. Nikhat Shaikh for their love and support during this whole research journey. Additionally, I am really very thankful to my main supervisor Prof. Dr. Abdul Latif bin Ahmad, and my co-supervisor Dr. Noorashrina binti A. Hamid for their appreciable supervision, valuable guidance and suggestions, and consistent support throughout my research.

I'd like to give special thanks to all the staff from management, laboratories, administration, and technical departments in School of Chemical Engineering for giving me guidance and support, especially to Nor Irwin Basir for sharing his previous experience related to my research and time to time support throughout the period. Also, I am grateful to all of my colleagues, friends and cousins for all of their moral support help and support throughout the research.

At last, but not least, I would like to express my gratitude to the Universiti Sains Malaysia for providing me such an outstanding research environment, facilities and more importantly, the USM fellowship. In addition, I am very grateful to Ministry of Higher Education Malaysia for their financial assistance through Fundamental Research Grant Scheme (FRGS) [203.PJKIMIA.6071355] during this research.

I would like to say Thank You to all of you for your support during this exceptional research experience, your support will be appreciated ceaselessly. Thanks a lot.

TABLE OF CONTENTS

ACKNOWLEDGEMENT	ii
TABLE OF CONTENTS	iii
LIST OF TABLES	xiii
LIST OF FIGURES	xvi
LIST OF ABBREVIATIONS	xix
LIST OF SYMBOLS	xv
ABSTRAK	xvi
ABSTRACT	xviii
CHAPTER 1: INTRODUCTION	
1.1 Introduction	1
1.2 Introduction of separators	3
1.3 Problem Statement	5
1.4 Research objective	7
1.5 Scope of research and limitations	8
1.6 Organization of thesis	8
CHAPTER 2: LITERATURE REVIEW	
2.1 Overview of separators	10
2.2 Polymer electrolyte membranes for lithium ion battery	11
2.2.1 Liquid polymer electrolyte membranes (LPEs)	14
2.2.2 Solid polymer electrolyte membranes (SPEs)	15
2.2.3 Gel-polymer electrolyte membranes (GPEs)	16
2.2.4 Composite membranes	19
2.3 Requirements of the separator	23
2.4 Preparation methods for GPEs (PEMs)	26
2.4.1 Casting technique	27
2.4.2 In situ polymerization	28
2.4.3 The inversion technique/phase separation	29
2.4.4 Electrospinning technology	30
2.4.5 Breath figure method	32

2.5	Introduction of the inorganic fillers	35
2.6	Electrochemical methods	41
2.6.1	Electrochemical impedance spectroscopy	41
2.6.2	EIS for battery equivalent circuit models	43
(a)	Electrical double layer capacitance, Cdl	43
(b)	Polarization resistance (Rp)	43
(c)	Diffusion and Warburg impedance (W)	44
(d)	Ohmic resistance (Ro)	44
(e)	Inductance (L)	45
2.7	Definitions	46
2.7.1	Internal resistance	46
2.7.2	Battery capacity	46
2.7.3	Current rate (C-rate)	46
2.7.4	Ionic conductivity	46
2.7.5	Energy density	47
2.8	Conclusions	47

CHAPTER 3: METHODOLOGY

3.1	Introduction	49
3.2	Chemicals and materials	49
3.3	Flow chart of experimental work	51
3.4	Description of major equipment	52
3.4.1	Glove box	52
3.4.2	Split test cell	54
3.4.3	Universal tensile strength tester	55
3.4.4	The electrochemical cell	56
3.5	Synthesis of particle and composite	58
3.5.1	Synthesis of Polyaniline (PANI) particles	58
3.5.2	Synthesis of PANI/graphene oxide (GO) composite	58
3.6	Synthesis of various PVDF-HFP membranes	59
3.6.1	Preparation of pristine PVDF-HFP membranes	59
3.6.2	Preparation of PVDF-HFP/PANI polymer electrolyte membrane	60
3.6.3	Preparation of PVDF-HFP/GO composite membrane	61
3.6.4	Preparation of PVDF-HFP/PANI/GO polymer electrolyte membrane	

		62
3.7	Physical Characterization	63
3.7.1	Membrane morphology	63
3.7.2	Porosity	64
3.7.3	Electrolyte Uptake (EU)	64
3.7.4	Functional Group Analysis	65
3.7.5	Thermal stability	65
3.7.6	Differential Scanning Calorimetry (DSC) Analysis	66
3.7.7	X-ray Diffraction (XRD) analysis	66
3.7.8	Membrane thickness and viscosity measurement	67
3.7.9	Mechanical stability	67
3.8	Electrochemical Characterization	68
3.8.1	Ionic conductivity	68
3.8.2	Linear sweep voltammetry (LSV) analysis	69
3.8.3	Chronoamperometry (CA) Analysis	70
3.8.4	Coin cell assembly	70
3.8.5	Coin cell testing	71
3.9	Electrochemical modelling through equivalent circuit models	72
3.9.1	Model validation and analysis	72

CHAPTER 4: RESULT AND DISCUSSION

4.1	Introduction	75
4.2	Effect of thickness and solvent variation on the performance of PVDF HFP membranes	76
4.2.1	Morphology of various PVDF-HFP membranes	76
4.2.2	Mechanical Strength Analysis	79
4.2.3	Conclusion	80
4.3	Effect of PANI addition on the performance of PVDF-HFP PEMs	81
4.3.1	Porosity and EU of PANI based PVDF-HFP PEMs	81
4.3.2	Scanning Electron Microscope (SEM) Analysis	82
4.3.3	Functional group analysis of PVDF-HFP/PANI membranes	84
4.3.4	Thermal stability of PANI based PVDF-HFP membranes	86
4.3.5	Mechanical strength of PANI based PVDF-HFP membranes	91
4.3.6	Ionic conductivity of PANI based PVDF-HFP membranes	92

4.3.7	Conclusion	93
4.4	Effect of graphene oxide on the performance of PVDF-HFP PEMs	94
4.4.1	Functional group analysis of PVDF-HFP/GO PEM	95
4.4.2	Porosity and EU of GO based PVDF-HFP PEMs	96
4.4.3	Thermal stability of GO based PVDF-HFP membranes	97
4.4.4	Mechanical strength of GO based PVDF-HFP membranes	101
4.4.5	Ionic conductivity of GO based PVDF-HFP membranes	102
4.4.6	Conclusion	103
4.5	Effect of PANI/GO on the performance of PVDF-HFP PEMs	104
4.5.1	Functional group analysis of PANI/GO membranes	105
4.5.2	Porosity and EU of PANI/GO based PVDF-HFP PEMs	107
4.5.3	Morphology of GO based PVDF-HFP PEMs	108
4.5.4	Thermal stability of PANI/GO based PVDF-HFP ternary membranes	110
4.5.5	Mechanical strength of PANI/GO based PVDF-HFP membranes	115
4.5.6	Ionic conductivity of PANI/GO based PVDF-HFP membranes.	117
4.5.7	Conclusion	118
4.6	PVDF-HFP/PANI/GO ternary hybrid polymer electrolyte membrane for lithium ion battery	119
4.6.1	Linear sweep voltammetry of optimum membranes	120
4.6.2	Chronoamperometry analysis of optimum membranes	121
4.6.3	Cycling performance of optimum PVDF-HFP PEMs	122
4.6.4	Electrochemical modelling of optimum PVDF-HFP PEMs	126
4.6.5	Conclusion	133

CHAPTER 5: CONCLUSION AND FUTURE PROSPECTS

5.1	Conclusions	134
5.2	Recommendations for future work	135

REFERENCES 137

APPENDICES

Appendix A: Pore size graphs/data obtained by Porolux

Appendix B: Different parametric values obtained for prepared PEMs

Appendix C: FTIR spectra of PVDF-HFP/GO

Appendix D: Screenshot of series IX software for tensile strength calculation

Appendix E: Pore size analysis

Appendix F: Sample calculations

LIST OF PUBLICATIONS

LIST OF TABLES

		Page
Table 1-1	Characteristics of secondary batteries	2
Table 1-2	General requirements of separators for LIBs	5
Table 2-1	The requirement of separator with brief explanations	24
Table 3-1	List of chemicals utilized for this research	50
Table 3-2	List of equipment utilized for membrane preparation and battery assembly	51
Table 4-1	Effect of solvent variation on porosity, thickness and viscosity of PVDF-HFP membrane	79
Table 4-2	Effect of thickness variation on porosity and mechanical strength of PVDF-HFP membrane	80
Table 4-3	Porosity and electrolyte uptake of pristine and PVDF-HFP/PANI membranes	82
Table 4-4	Characteristic peaks and possible assignments pristine PVDF-HFP and PVDF-HFP/PANI membranes	85
Table 4-5	T _m , T _d and X _c values of pristine and PANI based PVDF-HFP membranes	90
Table 4-6	Porosity and Electrolyte uptake of Pristine and PVDF-HFP/GO membranes	97
Table 4-7	T _m , T _d and X _c values of pristine and GO based PVDF-HF membranes	100
Table 4-8	Porosity and Electrolyte uptake of Pristine and PVDF-HFP/PANI/GO ternary hybrid membranes	107
Table 4-9	T _m , T _d and X _c values of pristine and PANI/GO based PVDF-HFP membranes	114
Table 4-10	Different EC models used for the EIS data obtained for pristine PVDF-HFP PEM	127
Table 4-11	The parameters obtained from R-CPE model fitting of optimum PVDF-HFP PEMs	131

LIST OF FIGURES

		Page
Figure 1-1	Schematic illustrating the mechanism of operation for a lithium ion battery	3
Figure 2-1	Various types of polymer electrolyte membranes	14
Figure 2-2	Schematic diagram and SEM image of an organic/inorganic trilayer separator. Reproduced with permission (Kim et al., 2010).	20
Figure 2-3	Sequence of stages resulting in the breath-figures self-assembly. A-D formation of the first row of pores. E-C Formation of the second row of pores. Reproduced with permission (Bormashenko, 2017).	34
Figure 2-4	Thermogravimetric curves of various polymer electrolyte membranes. Reproduced with permission (Kelley et al., 2012).	38
Figure 2-5	Electrochemical system of lithium ion battery at charging and discharging process	45
Figure 3-1	Schematic diagram of whole experimental work	52
Figure 3-2	The argon glove box	53
Figure 3-3	The split test cell coin cell assembly kit without crimping	55
Figure 3-4	Instron 3366 universal mechanical strength tester	56
Figure 3-5	The electrochemical cell (VMP3 analyzer)	57
Figure 3-6	Flow chart for synthesis of PVDF-HFP/PANI membrane	61
Figure 3-7	Schematic diagram of PVDF-HFP/GO membrane preparation	62
Figure 3-8	The schematic diagram of PVDF-HFP/PANI/GO ternary membrane preparation	63
Figure 3-9	Simple Randles's equivalent circuit	72
Figure 4-1	The SEM images of membrane surface and cross section 40:60 (a & b), 50:50 (c & d), 60:40 (e & f), 100:00 (g & h) of PVDF- HFP membranes	78

Figure 4-2	SEM images of surfaces (a & c) and (b & d) and cross sections (e) and (f) of pristine PVDF-HFP and PVDF-HFP/PANI membrane respectively	83
Figure 4-3	The FTIR spectra of pristine PVDF-HFP and PVDF-HFP/PANI membrane	86
Figure 4-4	Thermogravimetric (TGA) curves of PANI based PVDF-HFP membranes	87
Figure 4-5	Derivative of TGA curves (DTGA) of PANI based PVDF-HFP membranes	88
Figure 4-6	DSC curves of pristine and PANI based PVDF-HFP membranes	89
Figure 4-7	The XRD spectra of various PANI based PVDF-HFP membranes	91
Figure 4-8	Mechanical strength of PANI based PVDF-HFP PEMs	92
Figure 4-9	EIS complex graphs obtained for PANI based PVDF-HFP membranes	93
Figure 4-10	FTIR spectra of pristine PVDF-HFP and PVDF-HFP/GO membrane	96
Figure 4-11	Thermogravimetric (TGA) curves of GO based PVDF-HFP membranes	98
Figure 4-12	Derivative of Thermogravimetric (DTGA) curves (b) stability up to 400°C of pristine and GO based PVDF-HFP membranes	98
Figure 4-13	DSC curves of pristine and GO based PVDF-HFP membranes	99
Figure 4-14	XRD spectra of various GO based PVDF-HFP membranes	101
Figure 4-15	Mechanical strength of GO based PVD-HFP membranes	102
Figure 4-16	EIS complex graphs obtained for GO based PVDF-HFP membranes	103
Figure 4-17	FTIR spectra of various particles and different PVDF-HFP membranes	107
Figure 4-18	Pore size data of various PVDF-HFP PEMs	109

Figure 4-19	SEM images of surfaces (a)-(b), (d)-(e) and (g)-(h) and cross sections (c), (f) and (i) of pristine PVDF-HFP, PVDF-HFP/PANI and PVDF-HFP/PANI/GO membranes respectively	110
Figure 4-20	Thermogravimetric (DTGA) curves of PANI/GO based PVDF- HFP membranes	112
Figure 4-21	Derivative of Thermogravimetric (DTGA) curves of PANI/GO based PVDF-HFP membranes	112
Figure 4-22	The DSC analysis of pristine and PANI/GO based PVDF-HFP membranes	113
Figure 4-23	XRD spectra of various PANI/GO based PVDF-HFP membranes	115
Figure 4-24	Mechanical strength of PANI/GO based PVDF-HFP membranes	116
Figure 4-25	Ionic conductivity of PANI/GO based PVDF-HFP membranes	117
Figure 4-26	Linear sweep voltammetry analysis of optimum PVDF-HFP membranes	121
Figure 4-27	Lithium ion transference number Li^+ of optimum PVDF-HFP membranes	122
Figure 4-28	Charge-discharge curves of (a) pristine and (b) PANI based PVDF-HFP PEMs	124
Figure 4-29	Charge-discharge curves of (a) PVDF-HFP/GO and (b) PVDF- HFP/PANI/GO PEMs	125
Figure 4-30	Charge discharge curves of (a) charge discharge curve of PVDF-HFP/PANI/GO PEM and (b) rate performance of optimum PVDF-HFP PEMs	126
Figure 4-31	The Nyquist and Bode plot of R-C model fitting of pristine PVDF-HFP PEM	128
Figure 4-32	The Nyquist and Bode plot of R-L model fitting of pristine PVDF-HFP PEM	128
Figure 4-33	The Nyquist and Bode plot of R-CPE model fitting of pristine PVDF-HFP membrane	129

Figure 4-34	The Nyquist and Bode plots of PVDF-HFP/PANI membrane	130
Figure 4-35	The Nyquist and Bode plots of PVDF-HFP/GO membrane	131
Figure 4-36	The Nyquist and Bode plots of PVDF-HFP/PANI/GO membrane	132

LIST OF ABBREVIATIONS

Al ₂ O ₃	Aluminum oxide
ASTM	American society for testing and materials
CA	Chronoamperometry
DMC	Dimethyl carbonate
DSC	Differential scanning calorimetry
DTGA	Derivate of thermogravimetric
EC	Ethylene carbonate
EIS	Electrochemical impedance spectroscopy
FTIR	Fourier-transform infrared spectroscopy
GO	Graphene oxide
HCl	Hydrochloric acid
LiFePO ₄	Lithium iron phosphate
LiPF ₆	Lithium hexafluorophosphate
LPE	Liquid polymer electrolyte
LSV	Linear sweep voltammetry
MSE	Mean square error
NH ₄ OH	Sodium hydroxide
NMP	N-Methyl-2-pyrrolidone
PANI	Polyaniline
PE	Polyethylene
PMMA	Poly(methyl methacrylate)
PP	Polypropylene
PVAc	Polyvinyl acetate
PVDF	Poly(vinylidene) fluoride

PVDF-HFP	Poly(vinylidene fluoride-co-hexafluoropropylene)
PVDF-TrFE	Poly(vinylidene fluoride-co-trifluoroethylene)
SEM	Scanning electron microscopy
SiO ₂	Silicon dioxide
SPE	Solid polymer electrolyte
SPEEK	Sulfonated poly(ether ether ketone)
TGA	Thermogravimetric
TiO ₂	Titanium oxide
XRD	X-ray diffraction
ZrO ₂	Zirconium oxide

LIST OF SYMBOLS

ρ	Density of membrane (gm/cm ³)
A	Membrane diffusion area (cm ²)
C	capacitor
CPE	constant phase element
D_t	Membrane thickness (μm)
L	Inductor
R	Resistance (ohm)
V_d	Volume of membrane (cm ³)
W	Warburg constant
W_f	Weight of membrane after dipping it in electrolyte (gm)
W_i	Weight of membrane before dipping it in electrolyte (gm)
Y_f	Experimental values
Y_i	Predicted values

MEMBRAN HIBRID PERTIGAAN ELEKTROLIT POLIMER (PVDF-HFP)/PANI/GO UNTUK BATERI ION LITIUM

ABSTRAK

Poli (vinilidina hexafluoropropilina) PVDF-HFP merupakan komponen yang berpotensi sebagai pemisah dalam bateri ion litium kerana ketahanan kimianya yang sangat tinggi, kestabilan mekanikal dan haba yang besar beserta kos yang lebih rendah; walau bagaimanapun, komponen yang asalnya mempunyai ciri-ciri yang terhad dan memerlukan pengubahsuaian lanjut bagi mencapai prestasi yang diinginkan. Oleh itu, dalam penyelidikan ini, hibrid ternari PVDF-HFP/PANI/GO telah dibangunkan dan skop dibahagikan kepada tiga fasa yang pada permulaannya, dos polianilina (PANI) yang berbeza (1% berat, 2% berat, dan 3% berat) telah dicampur ke dalam matriks polimer PVDF-HFP bagi menghasilkan membran elektrolit PVDF-HFP/PANI dengan menggunakan kaedah nafas-bentuk. Penambahan PANI (2% berat) didapati mempengaruhi daya kekonduksian ionik di mana nilainya telah meningkat dari $1.98 \times 10^{-4} \text{ S cm}^{-1}$ bagi membran tunggal PVDF-HFP ke $1.04 \times 10^{-3} \text{ S cm}^{-1}$; walau bagaimanapun, kesan pengestrakannya mengakibatkan kekuatan tegangan membran tunggal PVDF-HFP menurun dari 4.2 MPa hingga 2.8 MPa.

Skop kedua, kesan grafina oksida (GO) dikaji dengan mevariasikan jumlah GO yang berbeza (1% berat, 2.5% berat dan 5% berat) ke dalam matriks polimer PVDF-HFP. Penambahan GO (2.5% berat) meningkatkan kekuatan tegangan membran PVDF-HFP dari 4.2 MPa hingga 12.5 MPa; walau bagaimanapun, ia menyebabkan kekonduksian ionik PEM tunggal diketepikan. Selanjutnya, bagi fasa ketiga, bahan komposit PANI/GO digabungkan atas faktor keunikan kedua-dua pengisi. PVDF-

HFP/ PANI hibrid ternari (2% berat)/GO (10% berat, 25% berat, dan 40% berat) PEM disintesis dan dicirikan untuk bateri ion litium.

Ternari PVDF-HFP/PANI/GO yang diperolehi menunjukkan peningkatan kekuatan tegangan sehingga 8.8 MPa. Tambahan pula, membran ternari PVDF-HFP/PANI/GO menunjukkan kestabilan terma yang luar biasa dengan T_d sehingga 498°C, peningkatan morfologi, pengambilan elektrolit tertinggi (367.5%) dan keliangan yang sangat baik sekitar 89%. Selain itu, PEM bagi PVDF-HFP tunggal, PVDF-HFP/PANI dan PVDF-HFP/PANI/GO yang optimum telah digunakan untuk pencirian elektrokimia dan pemodelan. Selain itu model R-CPE memberikan kualiti yang sesuai dengan nilai MSE sekitar 5% berbanding model R-C dan R-L. Seterusnya, PEM optimum yang disediakan berjaya digunakan dalam bateri ion litium dan menunjukkan kapasiti khusus yang baik untuk 10 pusingan permulaan. Walau bagaimanapun, PEM ternari PVDF-HFP/PANI/GO menghasilkan kestabilan yang lebih baik berbanding dengan PEM lain; oleh itu, ia diuji selanjutnya untuk pengejalan kapasiti dan ia mengekalkan kapasiti melebihi 95% selepas 30 kitaran. Kesimpulannya, penggunaan membran ternari PVDF-HFP/PANI/GO merupakan pemisah yang berpotensi bagi bateri ion litium di masa hadapan.

TERNARY HYBRID PVDF-HFP/PANI/GO POLYMER ELECTROLYTE MEMBRANE FOR LITHIUM ION BATTERY

ABSTRACT

Poly(vinylidene fluoride-co-hexafluoropropylene) PVDF-HFP is a promising candidate as a separator in lithium-ion batteries owing to its outstanding chemical resistance, high mechanical and thermal stability with lower cost; however, its pristine form has limited characteristics that require further modification to achieve enhanced performance. Therefore, in this research ternary hybrid PVDF-HFP/PANI/GO were developed and the scope was divided into three phases which at first, different dosages of polyaniline (PANI) (1 wt%, 2 wt%, and 3 wt%) are incorporated into PVDF-HFP polymer matrix to fabricate PVDF-HFP/PANI polymer electrolyte membrane by using breath-figure method. The PANI (2 wt%) inclusion influenced the ionic conductivity and enhanced it from $1.98 \times 10^{-4} \text{ S cm}^{-1}$ of pristine PVDF-HFP membrane to $1.04 \times 10^{-3} \text{ S cm}^{-1}$; however, its plasticizing effect resulted in tensile strength of pristine PVDF-HFP membrane from 4.2 MPa to 2.8 MPa.

Secondly, the effect of graphene oxide (GO) is investigated by varying different amount of GO (1 wt%, 2.5 wt%, and 5 wt%) into PVDF-HFP polymer matrix. The GO (2.5 wt%) addition remarkably enhanced the tensile strength of PVDF-HFP membrane from 4.2 MPa to 12.5 MPa; however, it showed negligible effect on ionic conductivity of pristine PEM. Therefore, in third phase, PANI/GO composite material is combined for the unique properties of both the fillers. The ternary hybrid PVDF-HFP/PANI (2 wt%)/GO (10 wt%, 25 wt%, and 40 wt%) PEMs are synthesized and characterized for lithium ion batteries.

The obtained PVDF-HFP/PANI/GO ternary membrane showed a remarkable improvement in tensile strength up to 8.8 MPa. Furthermore, the PVDF-HFP/PANI/GO ternary membrane exhibited outstanding thermal stability with T_d up to 498°C, improved morphology, highest electrolyte uptake (367.5%) and an excellent porosity of around 89%. Moreover, the obtained optimum pristine PVDF-HFP, PVDF-HFP/PANI, and PVDF-HFP/PANI/GO PEMs were considered for further electrochemical characterization and modelling. Also, the R-CPE model provided a best quality fit with MSE value of around 5% compared to R-C and R-L model. Further, the prepared optimum PEMs is successfully applied in lithium ion battery and showed good specific capacity for initial 10 cycles. However, PVDF-HFP/PANI/GO ternary PEM resulted in better stability compared to other PEMs; therefore, it is tested for capacity retention and it retained over 95% capacity after 30 cycles. In conclusion, the proposed PVDF-HFP/PANI/GO ternary membrane is a potential candidate as a separator in future lithium-ion batteries.

CHAPTER 1

INTRODUCTION

1.1 Introduction

World economy is highly dependent on fossil fuel and it has a severe impact on world ecology. Global climate impact and air quality are two major concerns about the fossil fuel. In addition, the increasing population in developing countries are enlarging their energy consumption and economies and is increasing dramatically. Therefore, electrochemical energy production has received great attention as an alternative source of energy due to its sustainability and environmentally friendly properties (Brownson et al., 2011; Li et al., 2014; Ntengwe, 2005; Rahman et al., 2014; Scrosati et al., 2011; Yu et al., 2016).

Batteries, fuel cells and supercapacitors are the systems for energy storage and conversion (Bruce et al., 2012; Choi et al., 2012; Han et al., 2014; Kim & Guiver, 2009, Makinouchi et al., 2017). The secondary batteries such as lithium-ion (LIBs), nickel-cadmium and lead-acid, etc. are rechargeable. Each battery has anode and cathode, electrolyte and separator. Anode is the negative electrode where the oxidation process occurs; while, the positive cathode electrode gains electron from external circuit. An electrolyte provides ionic conductivity between negative and positive electrodes. A separator is a physical barrier between electrodes to prevent short circuit while allowing ionic flow (Lu et al., 2015, Poullickas, 2013; Visco et al., 2009). LIB provides higher operating voltage, lower self-discharge, and higher coulombic efficiency compared to other batteries (Li et al., 2014; Speirs et al., 2014; Wang et al.,

2016; Yong et al., 2015). Some characteristics of the secondary batteries are listed in Table 1.1.

Table 1-1: Characteristics of secondary batteries (Yanilmaz, 2015)

Battery types	Voltage (V)	Energy Density (Wh/kg)	Power Density (Wh/kg)	Cycle life
Lithium ion	3.6	100-150	300	400-1.2k
Nickel-Cadmium	1.2	35-57	50-200	1k-2k
Lead acid	2	25-30	75-130	200-400
Nickel-Metal Hydride	1.2	50-80	150-250	600-1.5k

Figure 1.1 shows the schematic diagram of lithium ion battery which includes separator sandwiched in between lithium anode and carbon cathode; it provides superior properties compared to other secondary batteries such as higher working voltage, higher energy density, lower gravimetric density and longer service life. Owing to these properties, LIBs have been used in various devices such as eco-friendly transportation power storage, health care and defence (Lampič et al., 2016; Zhen et al., 2018; Scrosati et al., 2011). In addition, LIBs use lithium ions as the main charge carrier and maintain a high average discharge voltage of 3.7 V. Also, the LIBs are light in weight and can produce much high energy density compared to other batteries; therefore, it has become a promising choice for electric vehicles (EVs) (Yong et al., 2015). Lithium-ion batteries can be designed in various shapes such as prismatic, coin, pouch, and cylindrical depending on the devices and application areas. Cylindrical batteries are used in laptop computers, single-cell coin-shaped batteries are used in small electric appliances and portable IT devices, prismatic cells are common in

portable devices and pouch-shaped cells cased in aluminium plastic composites are good for electric vehicle applications (Lampič et al., 2016; Song et al., 2011). LIBs have received great attention since its introduction in 1990s due to high energy density, low gravimetric density, long cycle life and flexible design. The development of improved electrodes and separators for LIBs is critical to obtain high energy and power densities for electric and hybrid electric vehicles (Wang et al., 2016). Fast charging and discharging at high power rates, energy density, power, cycling, life, charge/discharge rates, safety and cost must be addressed to design advanced lithium-ion batteries.

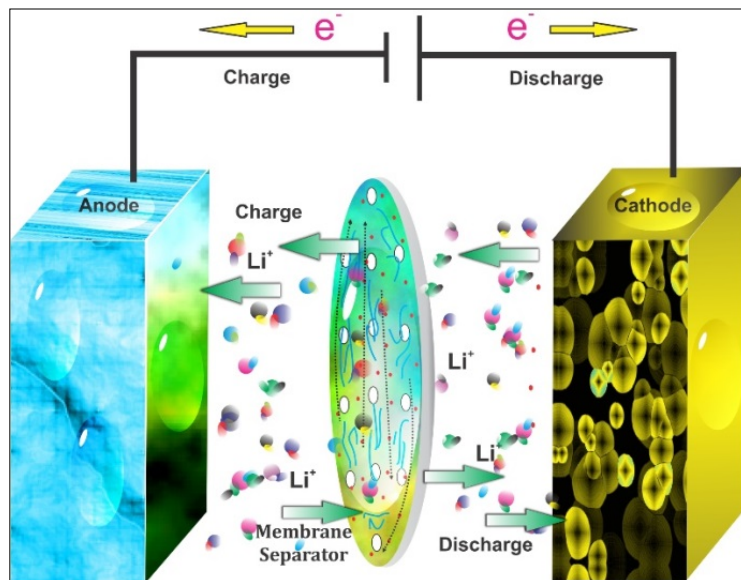


Figure 1-1: Schematic illustrating the mechanism of operation for a lithium-ion battery

1.2 Introduction of separators

A lithium ion battery (LIB) comprises of anode, cathode, separator and electrolyte. Separator is an essential component of LIBs that is placed between two electrodes to provide a physical barrier, while it serves as a medium for ion transfer at

the time of charging and discharging process. In production, some ionically conductive liquid electrolyte is used to fill the pores of the separator (Liu et al., 2017). The separator plays an important role in LIBs; it avoids the electronic contact and serves as a medium for ion transport between negative and positive electrodes; also, it provide and maintain a good support to the electrode, offers better ionic impedance at higher temperatures, and hold the electrolyte effectively for a longer time. For the accomplishment of these features, the separators need to be electrochemically and chemically stable towards the electrolytes and the electrodes; also, it must have an excellent thermal and mechanical stability to withstand at elevated temperature and at high tension during battery assembly and a charge-discharge process (Costa et al., 2013; Deimede & Elmasides, 2015; Jeong et al., 2012). Even though the separator does not participate in any cell reactions, the materials and structure of the separators affect the performance of LIBs. The separator influences internal cell resistance and cell kinetics so that it affects the performance of battery such as cycle life, energy density, power density, and safety.

Polymer electrolyte membranes (PEMs) have been extensively used as a separator in lithium ion batteries. The various types of PEMs such as solid polymer electrolyte membranes (SPEs), liquid polymer electrolyte membranes (LPEs), gel polymer electrolyte membranes (GPEs) etc. have received tremendous attention in the last couple of decade. Each separator is different and has its own merits and demerits and the selection of separators affects the performance of lithium-ion batteries. Many factors must be considered while choosing the separators for LIBs. General requirements are summarized below in Table 2 and detailed description was provided in the upcoming section.